The beginning of branching behaviour of vortex-induced vibration during two-dimensional flow

J.S. Leontini[*], M.C. Thompson, K. Hourigan

Fluids Laboratory for Aeronautical and Industrial Research (FLAIR), Department of Mechanical Engineering, Monash University, Wellington Rd., Clayton, Victoria, 3800, Australia

Abstract

To date, the majority of studies of vortex-induced vibration (VIV) of a cylinder constrained to oscillate transverse to the freestream have been experimental, and at a Reynolds number, Re, where the flow is inherently three-dimensional. At these higher Re, an upper and lower branch of response are observed. Mostly, these branches have not previously been investigated at lower Re where the flow is two-dimensional. Therefore, two-dimensional simulations have been performed at Re = 200 to thoroughly investigate the response of a cylinder to VIV. It was found that two regimes of response were present, similar in nature to the upper and lower branch at higher Re. While some differences were present, it was found that the genesis of the higher-Re flow behaviour was present in the low-Re two-dimensional flow, with evidence for this found in the amplitude, frequency and phase response of the cylinder.
© 2006 Elsevier Ltd. All rights reserved.

1. Introduction

There is a large body of work pertaining to elastically mounted cylinders constrained to oscillate transverse to a free stream. Early work in this area (Feng, 1968; Sarpkaya, 1979; Bearman, 1984) concentrated on areas of practical engineering importance, such as magnitudes of oscillation and the forces involved therein.

More recent work in this area has been focused on classifying different regimes of synchronous response, and attempting to explain the differences between them. This classification work began with the work of Khalak and Williamson (1996) and has continued with the contributions of Khalak and Williamson (1999) and Govardhan and Williamson (2002). The main conclusion from this work is that there exist two synchronous response "branches", termed the upper and lower branch. The upper branch is characterized by phase angles between lift force and displacement of close to zero, a primary oscillation frequency of close to the natural frequency of the cylinder system, and peak amplitudes of oscillation that can exceed one cylinder diameter. The lower branch is characterized by lower amplitudes of oscillation than the upper branch (hence the names 'upper' and 'lower branch'), phase angles of close to 180°, and slightly higher oscillation frequencies. Both exhibit the 2P shedding mode (Williamson and Roshko, 1988), but this mode is more obvious in the lower branch.

All of the aforementioned work involved experiments with Reynolds number Re > 1250, where Re = UD/v, with U the freestream velocity, D the cylinder diameter, and v the kinematic viscosity. The vast majority of

---

[*]Corresponding author. Tel.: +61 3 9905 1573; fax: +61 3 9905 3122.

E-mail address: justin.leontini@eng.monash.edu.au (J.S. Leontini).

studies of these branches have also been performed at Re > 1250 [see reviews by Sarpkaya (2004), and Williamson and Govardhan (2004)], where the flow is inherently three-dimensional. Only one experimental study has been performed at Re < 150 to help quantify the effect of this three-dimensionality (Anagnostopoulos and Bearman, 1992).

While only a single set of low-Re experiments has been performed, the low-Re problem has been studied using two-dimensional simulation (Blackburn and Karniadakis, 1993; Blackburn and Henderson, 1996). These studies showed a reduced range of reduced velocities for significant amplitude response and a lower maximum amplitude [$\simeq 0.6$, similar to the low-Re experimental maximum of Anagnostopoulos and Bearman (1992)]. This lower peak response is clearly demonstrated in the "Griffin" plot of Govardhan and Williamson (2000), where peak amplitude is plotted against a combined mass-damping parameter. All simulations or experiments at Re where the flow is two-dimensional showed lower peaks, leading Govardhan and Williamson (2000) to conclude this was a Reynolds number effect, and also leading them to imply that the upper branch does not occur at low Re, where the flow is two-dimensional. This conclusion seems to be supported by the work of Blackburn et al. (2000), in which both two-dimensional and limited three-dimensional simulations, as well as experiments, were performed at similar conditions. The three-dimensional simulations matched the experiments well, whereas no amplitude branches were observed for the two-dimensional simulations. This also led to the conclusion that two-dimensional simulations were inadequate for modelling higher-Re vortex-induced vibration (VIV).

It is conjectured here that, while two-dimensional simulations cannot faithfully model the flow at Re > 300, where the flow is inherently three-dimensional, valuable information can be gained from simulations at Re where the flow is two-dimensional that is still relevant at higher Re where the flow is three-dimensional. It is shown here that the first stages of the upper and lower branch behaviour can be observed in two-dimensional simulations at Re = 200, with supporting evidence from the frequency, total phase, and instantaneous amplitude and phase behaviour. The timing of vortex-shedding is also briefly investigated. It is concluded that the mechanism that causes the upper and lower branches is not a product of three-dimensionality, although it may be amplified by three-dimensionality. It is hoped that this can contribute not only to the increasingly important problem of low-Re VIV, but also to the understanding of the causes underlying the higher-Re VIV behaviour.

2. Computational method

The incompressible Navier–Stokes equations were solved in an accelerated frame of reference attached to the cylinder. An extra noninertial forcing term was introduced into the momentum equation which represented the acceleration of the reference frame.

Due to the coupling between the fluid and the structural response of the cylinder, the convection term was treated semi-implicitly. This was done by iterating through the three substeps (diffusion, pressure, and convection) and the harmonic motion equation governing the structural response until the velocity and pressure fields, and cylinder motion converged. Further details of the time-splitting method can be found in Karniadakis et al. (1991) and Thompson et al. (1996).

A spectral-element technique was employed on a 508 macro-element mesh, with the majority of elements in the boundary layer and wake regions. The geometry was split into quadrilateral elements, and within these elements the velocity and pressure fields were represented by eighth-order tensor-product polynomials, associated with Gauss–Lobatto–Legendre quadrature points. Details of this approach and implementation can be found in Thompson et al. (1996). Freestream boundary conditions were applied at the inlet and sides of the computational domain, a no-slip boundary was applied at the cylinder surface, and the normal velocity gradient set to zero at the outlet.

3. Results

All of the results presented herein were obtained at Re = 200, and at a mass ratio of $m^* = m/m_f = 10$, where m is the mass of the cylinder system and m_f is the mass of displaced fluid. The damping ratio, $\zeta = c/c_{\text{crit}}$, where c is the damping coefficient, was set to $\zeta = 0.01$, resulting in a combined mass-damping of $m^*\zeta = 0.1$. The use of a combined mass-damping parameter has been shown to be of use down to very low values (Naudascher and Rockwell, 1994).

3.1. Ranges of response regimes

The top plot of Fig. 1 shows $A^*_{\max}$ versus U^*, where $A^* = A/D$ with A the amplitude of response, and $U^* = U/f_N D$ and f_N is the cylinder natural frequency in the fluid, assuming an inviscid added-mass term applies. Inspection of this plot shows no evidence of branching in the high-amplitude region, but instead shows a single contiguous variation with slowly decreasing amplitude. The same plot of experimental results, as found in Khalak and Williamson (1999), clearly shows the upper and lower branches.

However, this does not mean that there are not two branches present in the two-dimensional flow. The second plot of Fig. 1 shows the peak lift coefficient, $C_{L\max}$ versus U^*, where $C_L = F_{\text{lift}}/0.5\rho U^2 D$ and F_{lift} is the instantaneous lift force per unit length and ρ is the fluid density. This figure shows that the highest lift forces are experienced when $4.2 < U^* < 4.7$ and that a sudden drop in the peak lift force is experienced at the upper limit of this range. This indicates that while there is not a great change in the peak amplitude of oscillation, there is a change in the very character of the flow.

More evidence of this change of character is shown in the third plot of Fig. 1 where the standard deviation, σ, of the amplitude envelope obtained using a Hilbert transform [as described by Khalak and Williamson (1999)] plotted against
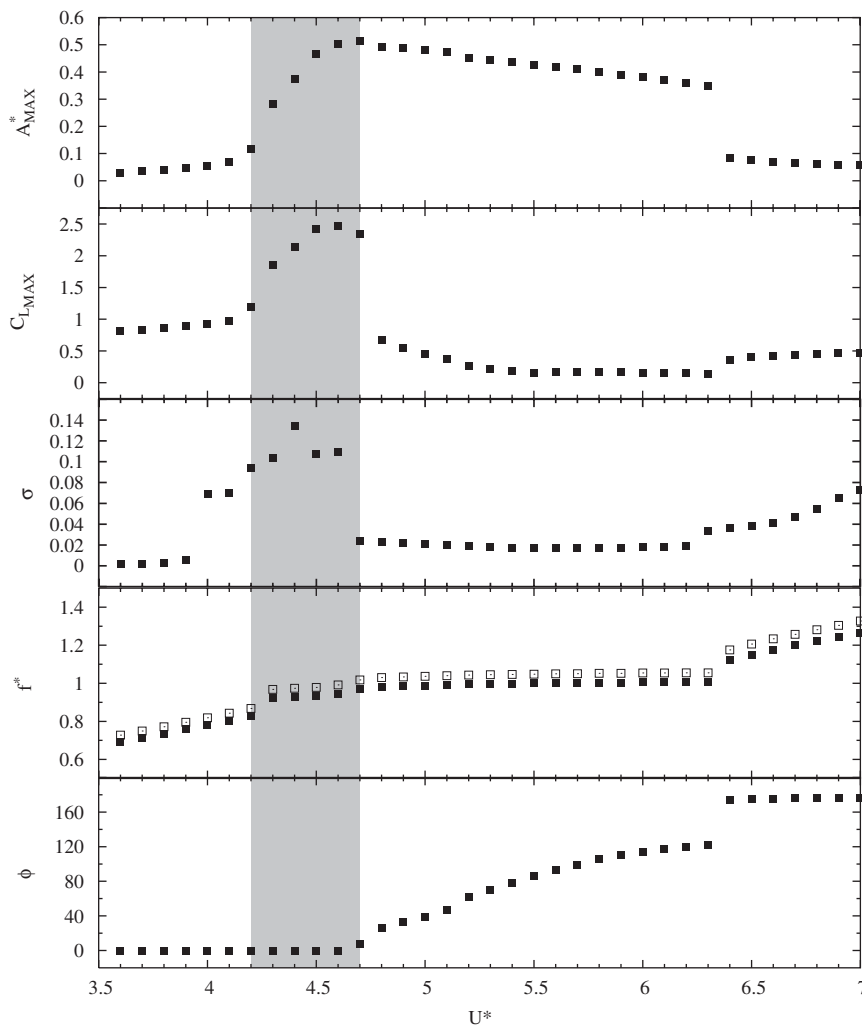

Fig. 1. Response for the elastically mounted cylinder for $m^* = 10$. From the top plot down: $A^*_{\max}$; $C_{L\max}$; σ, the standard deviation of the amplitude envelope obtained using a Hilbert transform; f^*, normalized by $f_{N_{\text{fluid}}}$ (□) and $f_{N_{\text{vac}}}$ (■); ϕ, the average phase between lift force and cylinder displacement. All are plotted versus U^*. All parameters except for $A^*_{\max}$ show a distinct branch of response for $4.2 < U^* < 4.7$ shown by the shaded strip.

U^*. This shows that for $U^* > 4.7$ in the high-amplitude regime the amplitude is very constant (indicated by the fact that $\sigma \simeq 0$). However, in the range $4.2 < U^* < 4.7$, σ is significantly higher, indicating the amplitude varies over the history of the flow. These extra pieces of information related to the amplitude of response show that while the peak amplitude does not vary discontinuously over the high-amplitude regime, there are indeed two regions where the flow dynamics are considerably different.

Other parameters, besides amplitude, show the same dual-regime behaviour. The fourth plot of Fig. 1 shows f^* plotted against U^*, where $f^* = f/f_N$ and f is the primary frequency of response. The primary frequency of response was defined as the frequency with the highest energy content from a spectrum of the response. Although only one frequency is plotted for each value of U^*, this should not be interpreted as if only this frequency is present in the response. In fact, over the range $4.2 < U^* < 4.7$, multiple frequencies are present, and the spectra of response become more noisy with increasing U^* in this range. Similar behaviour was observed by Blackburn and Henderson (1996) in their chaotic regime. This plot shows that in the range $4.2 < U^* < 4.7$ the primary frequency of response is consistently lower than when $U^* > 4.7$. A similar step in frequency is seen in the transition from the upper to lower branch at higher Re in the experiments of Khalak and Williamson (1999). With this step in primary frequency, the spectrum of frequencies present in the results also dramatically decreases, with effectively only a pure-tone response observed in the lower-type branch. Also plotted on the same axes is f^*, but normalized by the natural frequency in vacuo. It is shown that in the high-amplitude regime, the frequency of response approaches the natural frequency in a vacuum.

A change in average phase behaviour is also observed as U^* is increased beyond $U^* = 4.7$, as shown in the fifth plot of Fig. 1. In the upper-type branch, where $4.2 < U^* < 4.7$, the average phase, ϕ_{ave} is approximately $0°$, whereas an almost linear increase is observed in ϕ_{ave} with increasing U^* in the lower-type branch. It is conjectured that this increase is due to a gradual change in the vortex-shedding timing. This conjecture is further investigated in Section 3.3. Higher-Re experiments also uncover a change in average phase behaviour with the transition from the upper to lower branch. However, experiments reveal a sudden jump in average phase of around $180°$, rather than the gradual climb observed here. Still, it is of note that both the higher-Re experiments and low-Re simulations show a distinct change in phase behaviour over the high-amplitude region.

All of the parameters plotted in Fig. 1 show a high-amplitude regime, where the amplitude of response is significant, and the shedding frequency moves away from f_{St}, the shedding frequency of a fixed cylinder, towards f_N. Except for the peak amplitude of response, all these parameters show that this high-amplitude regime can be divided into two regions with distinct behaviour, with the transition between the two "branches" occurring around $U^* \simeq 4.7$. Similar results were obtained by Blackburn and Henderson (1996). They too observed two regions over the high-amplitude regime, that they dubbed the chaotic regime and the synchronized regime, coinciding with the upper-type and lower-type branches here. Similar trends in the mean amplitude, lift coefficient and frequency were observed during that study to those presented here.

The plot in Fig. 1 of σ against U^* here further reinforces the fact that the response in the upper-type branch is far from settled, and varies considerably over time. This variation is not even quasi-periodic, as the results in the following section further demonstrate. Also, inspection of this plot along with the plot of A^*_{max} shows that it is in the region where the amplitude is varying that the highest peak amplitudes are obtained.

Another unique result of this study is the plot in Fig. 1 of the average phase ϕ against U^* for two-dimensional flow at low Re. This plot shows that although the flow throughout the upper-type branch can be described as chaotic, its average phase is very close to zero. While this information can be valuable, it can be misleading to represent parameters such as phase and frequency of oscillation by a single number, when such variation occurs. Therefore, examples of the temporal variation of ϕ are presented in the following section for cases in both the upper-type and lower-type branch.

3.2. Instantaneous behaviour

As well as changes in the time-averaged behaviour, the behaviour of the flow over time is distinctly different in the upper-type branch compared to the lower-type branch. The upper-type branch is far from purely periodic, with large variations in the oscillation characteristics over time. This branch also realizes the largest amplitudes of oscillations and lift forces.

The amplitude history for $U^* = 4.6$, in the middle of the upper-type branch, is presented in the first plot of Fig. 2. Inspection of this figure shows that while the peak amplitude reached is near the maximum peak amplitude for any value of U^*, the peak amplitude is only experienced intermittently. An almost-repetitive growth and decay cycle is experienced that results in the higher values of σ plotted in Fig. 1.

The second plot of Fig. 2 shows the instantaneous phase, ϕ, over time, obtained through the use of a Hilbert transform, for $U^* = 4.6$. It shows that while the average phase is close to zero, the phase is highly mobile, varying in line
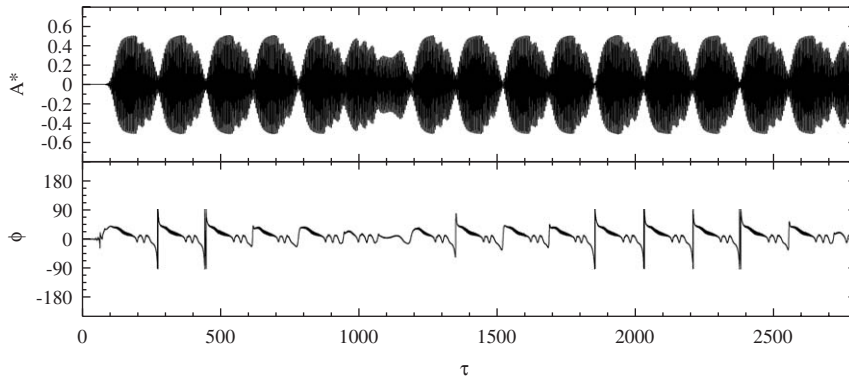
Fig. 2. Displacement history (top) and phase history (bottom) obtained using a Hilbert transform when $U^* = 4.6$, $m^* = 10$.
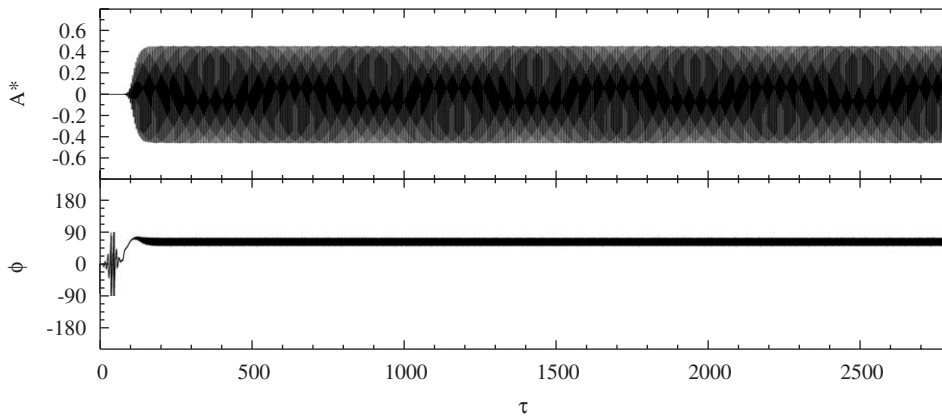

Fig. 3. Displacement history (top) and phase history (bottom) obtained using a Hilbert transform when $U^* = 5.2$, $m^* = 10$.

with the growth and decay of amplitude. It is unclear whether the amplitude controls the phase or the phase controls the amplitude, with the two seeming to be coupled and each taking precedence at different times in the growth–decay cycle.

This variation disappears with transition to the lower-type branch. Fig. 3 shows the amplitude and phase history when $U^* = 5.0$. The amplitude of oscillation is constant, and follows a sinusoidal history. Inspection of the phase history clearly shows that all the variation present in the upper-type branch has been eliminated, with no growth–decay cycle and a very constant phase.

While the growth and decay cycle present at $U^* = 4.6$ seems almost regular, it seems to be more than just a superposition of frequencies causing beating. It is due to the interaction and coupling of the phase of shedding and the amplitude of oscillation. This process is explained with reference to Fig. 4. Fig. 4(a) shows the wake when the amplitude of oscillation is small, at $\tau = 300$, where $\tau = tU/D$ is nondimensionalized time. The wake formed is narrow and the shed vortices almost take on a single-row configuration.

Due to resonance, the oscillation grows over time, altering the timing of vortex-shedding and the wake configuration. Fig. 4(b) shows the wake at $\tau = 350$. The shed vortices take on a double-row configuration very close to the rear of the cylinder.

The lateral spacing of the vortices in the double-row configuration continues to grow with increasing amplitude of oscillation. This trend continues until a critical amplitude is reached. The critical amplitude in this situation is defined as the amplitude at which the phase can no longer vary smoothly with increasing amplitude, and a sudden shift in phase of vortex-shedding of around $180°$ occurs. This is realized as a sudden shift of the side of the cylinder from which vortices are shed at a given point in the oscillation cycle. This sudden shift causes the wake to quickly become disordered, as is observed in Fig. 4(c), at $\tau = 416$.

The process of intermittent stages of order, with the wake approaching synchronization, and then disorder was mentioned by Blackburn and Henderson (1996). The disordering of the wake causes a drop in lift force which causes a
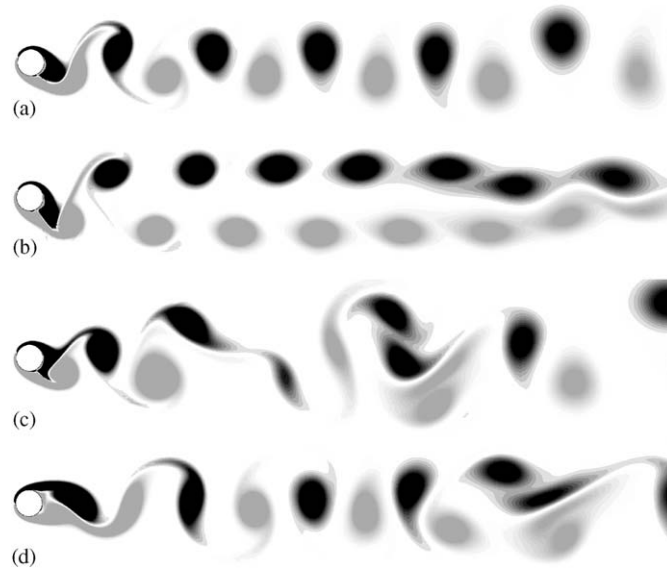
Fig. 4. The evolution of the wake over time when $U^* = 4.6$, $m^* = 10$. (a) With the amplitude of oscillation near its minimum at $\tau = 300$, the wake takes on a single-row configuration. (b) The amplitude of oscillation grows and the wake takes on a double-row configuration such as this image taken at $\tau = 350$. (c) At $\tau = 416$ the wake quickly becomes disordered. (d) With the amplitude now greatly reduced, the wake reverts to an organized single-row configuration, as it has in this image at $\tau = 450$.

drop in oscillation amplitude. With the amplitude of oscillation reduced, the wake regains its order, again in the single-row configuration, as can be seen in Fig. 4(d). From this single-row configuration, the growth–decay cycle is free to commence again.

3.3. Phase of shedding and vortex timing

As previously mentioned, the growth–decay cycle scenario does not occur in the lower-type branch. Instead, for a given U^*, the amplitude of oscillation and ϕ, the phase between lift force and displacement, are constant over time. While these quantities are fixed for a given U^*, a smooth variation in both the A^* and ϕ is seen with increasing U^*, as re-examination of Figs. 1(a) and 1(e) will reveal.

As the mass ratio, $m^* = 10$, used throughout this study is relatively high, the added mass force will play a lesser role than the vortex force, as defined by Govardhan and Williamson (2000) and Carberry et al. (2003). Therefore, the overall phase will be primarily governed by the phase of vortex-shedding, or the timing of vortex-shedding with respect to the oscillation cycle.

From the phase results shown in Fig. 1(e), it would therefore be expected that a gradual change in vortex-shedding timing would be observed with increasing U^*. This is, in fact, what is observed, as is illustrated in Fig. 5.

Fig. 5 shows instantaneous wake images for $U^* = 5.0$, 5.2, 5.4 and 5.6. At $U^* = 5.0$, with the phase near $0°$, the shed vortices take on a stable double-row configuration close to the rear of the cylinder. Increasing U^* to $U^* = 5.2$ sees the phase ϕ increase, and the wake narrows, with the vortices forming into the double-row configuration approximately three shedding cycles downstream. A further increase to $U^* = 5.4$ sees a further increase in phase, which further delays the formation of the double-row configuration. With an increase to $U^* = 5.6$, a single-row vortex formation is seen to persist for the entire length of the computational domain.

Interestingly, these stable intermittent phases of shedding are not observed in higher-Re experiments, as the phase jumps relatively suddenly from $\simeq 0°$ to $\simeq 180°$ on transition from the upper to the lower branch (Khalak and Williamson, 1999). The cause of this difference remains open to investigation.

3.4. Comparisons with branching at higher Reynolds number

From the results of the previous sections, it is clear that there are two regimes of high-amplitude response with respect to U^* when the flow is two-dimensional. Traditionally, the designations of upper and lower branches has been given to
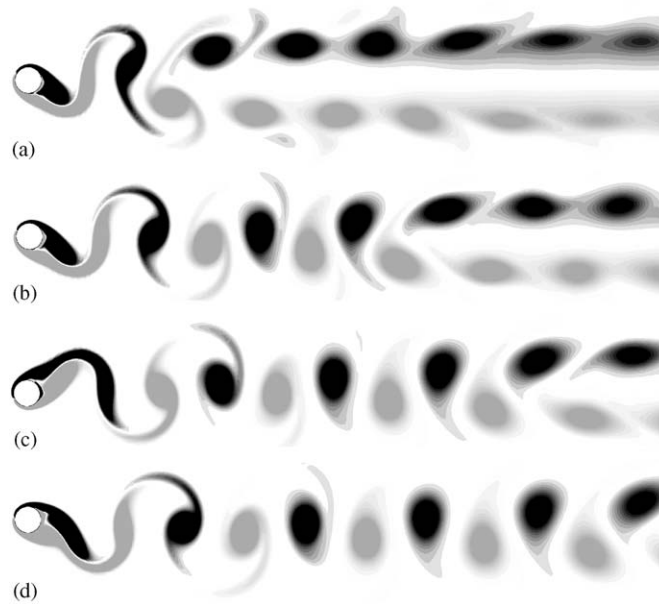
Fig. 5. Wake evolution as a function of U^* in the lower-type branch: (a) $U^* = 5.0$ sees the shed vortices quickly arrange themselves into a double-row configuration, (b) $U^* = 5.2$ sees the formation of the double-row configuration to be delayed, (c) $U^* = 5.4$ sees the double-row configuration further delayed as the phase of shedding increases, (d) $U^* = 5.6$ results in the single-row configuration persisting much further downstream.

results from higher-Re experiments, where the peak amplitude response differs between the two branches. However, many similarities exist between the two-dimensional and three-dimensional flow that suggests the double-branched behaviour persists in both situations.

Firstly, it is reported that the upper branch in experiments is quite sensitive and unstable, often with it being observed in intermittent bursts intermingled with periods of lower branch oscillation (Khalak and Williamson, 1999). The results from Blackburn and Henderson (1996) and the extended results of the current study indicate that the upper-type branch in two-dimensional flow is chaotic, with the amplitude of oscillation varying over time. Therefore, this intermittency of the amplitude of response in the upper branches is shared between the two-dimensional and three-dimensional flow. Leading on from this, Khalak and Williamson (1999) also noted that the lower branch is much more stable, and "remarkably" periodic. The results of this study show that the lower-type branch is also periodic, with literally no deviation from a pure sinusoid seen in the amplitude response of the cylinder.

Secondly, the upper branch typically occurs over a narrow band of U^*, at values of U^* lower than those where the lower branch occurs. The same behaviour, with respect to the ordering of the branches in terms of U^*, is observed in the current results for the two-dimensional flow.

Thirdly, the lower branch during experiments results in a 2P wake mode that is periodic. The two-dimensional flow lower-type branch results in a 2S wake mode. *A priori*, this seems to be a major point of difference. However, the 2P wake mode (if a spanwise mean is taken) and the 2S mode of the two-dimensional flow share the same symmetry group, Z_2, consisting of a half-period evolution and a spatial reflection about the wake centreline. Also, the 2S wake of the two-dimensional flow can be very wide, meaning the only difference is that the vortical structures of the 2S wake do not split in the near wake, as they do for the 2P wake (Govardhan and Williamson, 2000).

All of these similarities taken together seem to suggest that the beginning of the branching behaviour present in the three-dimensional flow may have its roots in the two-dimensional flow.

4. Conclusions

It has been shown that even for low-Reynolds number two-dimensional flow, two regimes of synchronized response exist during VIV. These regimes bear some resemblance to the upper and lower branch found in higher Re experiments where the flow is inherently three-dimensional. Evidence for these regimes at low Re is not apparent in the peak

amplitude of response, but is evident in the observed variation in amplitude over time. It is also found by examining the magnitude of the lift force, the variation in primary oscillation frequency, and the variation in the phase between the lift force and displacement with increasing U^*. The similarities between the two-dimensional and three-dimensional flow behaviour suggests that the three-dimensional flow branching behaviour has its genesis in the two-dimensional flow.

These observations shed light on the problem of low-Re VIV. They also suggest that the branching behaviour that is so obvious at higher Re is not caused by the presence of three-dimensionality, but is enhanced by it.

Acknowledgement

References

Anagnostopoulos, P., Bearman, P., 1992. Response characteristics of a vortex-excited cylinder at low Reynolds numbers. Journal of Fluids and Structures 6, 39–50.

Bearman, P., 1984. Vortex shedding from oscillating bluff bodies. Annual Review of Fluid Mechanics 16, 195–222.

Blackburn, H., Henderson, R., 1996. Lock-in behaviour in simulated vortex-induced vibration. Experimental Thermal and Fluid Science 12, 184–189.

Blackburn, H., Karniadakis, G., 1993. Two- and three-dimensional simulations of vortex-induced vibration of a circular cylinder. In: Proceedings of the Third International Offshore and Polar Engineering Conference, Singapore.

Blackburn, H., Govardhan, R., Williamson, C., 2000. A complementary numerical and physical investigation of vortex-induced vibration. Journal of Fluids and Structures 15, 481–488.

Carberry, J., Sheridan, J., Rockwell, D., 2003. Controlled oscillations of a cylinder: a new wake state. Journal of Fluids and Structures 17, 337–343.

Feng, C., 1968. The measurement of vortex-induced effects in flow past stationary and oscillating circular and D-section cylinders. Master's Thesis, University of British Columbia, Canada.

Govardhan, R., Williamson, C., 2000. Modes of vortex formation and frequency response of a freely vibrating cylinder. Journal of Fluid Mechanics 420, 85–130.

Govardhan, R., Williamson, C., 2002. Resonance forever: existence of a critical mass and an infinite regime of resonance in vortex-induced vibration. Journal of Fluid Mechanics 473, 147–166.

Karniadakis, G.E., Israeli, M., Orszag, S.A., 1991. High-order splitting methods of the incompressible Navier–Stokes equations. Journal of Computational Physics. 97, 414–443.

Khalak, A., Williamson, C., 1996. Dynamics of a hydroelastic cylinder with very low mass and damping. Journal of Fluids and Structures 10, 455–472.

Khalak, A., Williamson, C., 1999. Motions, forces and mode transitions in vortex-induced vibrations at low mass-damping. Journal of Fluids and Structures 13, 813–851.

Naudascher, E., Rockwell, D., 1994. Flow-Induced Vibrations: An Engineering Guide. A.A. Balkema, Dordrecht.

Sarpkaya, T., 1979. Vortex-induced oscillations: a selective review. Journal of Applied Mechanics 46, 241–258.

Sarpkaya, T., 2004. A critical review of the intrinsic nature of vortex-induced vibrations. Journal of Fluids and Structures 19, 389–447.

Thompson, M., Hourigan, K., Sheridan, J., 1996. Three-dimensional instabilities in the wake of a circular cylinder. Experimental Thermal and Fluid Science 12, 190–196.

Williamson, C., Govardhan, R., 2004. Vortex-induced vibrations. Annual Review of Fluid Mechanics 36, 413–455.

Williamson, C., Roshko, A., 1988. Vortex formation in the wake of an oscillating cylinder. Journal of Fluids and Structures 2, 355–381.